Proceedings World Geothermal Congress 2010
Bali, Indonesia, 25-29 April 2010

Development Implications Arising from the Reinterpretation of the Results of a 3D MT Inversion at Bedugul, Bali, Indonesia

Ian Bogie[1], Edwin J. Joenoes[2], Shanti R. A. Sugiono[3], Stephen Hallinan[4] and Don Watts[4]

[1]SKM, PO Box 9806, Newmarket, Auckland, New Zealand

[2]Bali Energy Ltd.

[3]Star Energy Holdings Ltd.

[4]Geosystem Srl - Western Geco

ibogie@skm.co.nz, shanti.sugiono@starenergy.co.id,

Keywords: Bali, Bedugul, geothermal, caldera, MT, pull-apart

ABSTRACT

Exploration drilling in 1997-1998 of the Bedugul geothermal field in Bali discovered a deep, but hot, exploitable geothermal reservoir. However, the wells are poorly permeable. A 3D MT inversion has been reinterpreted in light of the results from the wells in order to further assess the field. The general resistivity pattern of geothermal fields in andesitic terranes is found. A near surface high resistivity layer overlies a shallow conductor that wraps around a moderately resistive core. A fainter repeat of this pattern towards the northeast above a gravity high along the trend of younger volcanism may represent an older, colder geothermal system in this direction. In the hot system to the southwest an elongate southeast trending higher resistivity zone in the conductor to the northwest may represent the recharge zone. Another southeast elongate zone further south may represent the outflow; given that the majority of the system's surface thermal features lie in this direction. The two southeast trending zones are offset in a fashion suggestive of a pull-apart feature between them. If this is the case it could form a broad permeable zone in which the field could be developed.

1. INTRODUCTION

The Bedugul geothermal project is located within the Bratan caldera in Bali, Indonesia (Figure 1). The area was originally explored by Pertamina (Mulyadi and Hochstein, 1981; Soetantri and Prijanto, 1982) who entered into a JOC with California Energy in 1995. California Energy as Bali Energy Ltd. conducted further exploration that culminated in the drilling of three deep wells (BEL 01, BEL-02 and BEL-03) in 1997-1998. The initial work undertaken by California Energy established that an exploitable geothermal system is present, by drilling wells into a high temperature reservoir that contains near neutral-pH water. The size of the system was partially defined by a corehole program, but the results were not in good agreement with the original interpretation of the MT (magnetotellurics). The exact size and location of the resource were thus not well defined.

The project was halted in response to the 1998 Asian financial crisis. Bali Energy Ltd as a reconstituted entity took over the project in 2002. The two deep wells capable of discharge (BEL-02 and BEL-03) were flow tested (Hochstein *et al*., 2005; Mulyadi *et al*., 2005) and earlier MT work was reworked as a 3D inversion in 2004 (Geosystem, 2004), unfortunately this was not in time to be included in the WGC 2005 paper of Mulyadi *et al*., (2005). This paper reports a further reinterpretation of this work made in 2009.

2. WELL MEASUREMENT BACKGROUND

Temperature and pressure measurements in the wells are suggestive that BEL-02 (Figure1) is nearest the system's upflow. The evidence for this are the higher pressures and temperatures for elevation (and these temperatures are high: > 320°C) close to the bottom of BEL-02 in comparison to BEL-03. No pressure profiles are available for BEL-01 as it had to be abandoned with a fish in it. Temperatures in this well were only measured while the rig was on the hole, but the latest obtained were sufficiently high to suggest they may be at least partially stabilized. The highest measured temperature (345°C at -1000 m asl) in BEL-01 is less than the temperature in BEL-02 extrapolated to this depth and thus BEL-01 is likely to be further from the upflow. The high temperatures would also suggest that the system retains relatively high temperatures for depth away from the upflow. The pressure gradient from BEL-02 to BEL-03 suggests a general southerly flow.

The pre-discharge pressure profiles indicate the presence of a liquid reservoir in both wells. However, upon discharge BEL-02, after a very short period of two-phase production, produced only steam and BEL-03 has an enthalpy (2620 $kJKg^{-1}$) much higher than that of liquid water at its feed zone temperature (1800 $kJKg^{-1}$). These results, in combination with the strong silica saturation, the disparity between silica and cation geothermometry, high gas content (5 wt%) and low CO_2/H_2S ratio (Mulyadi *et al*., 2005) indicate that both wells are not very permeable and isothermal boiling is occurring in the surrounding formation. Nevertheless, once excess enthalpy has been corrected for, the reservoir Cl concentration of BEl-03 water is only 2,500 mg/l. This is low in comparison to water-dominated geothermal systems in andesitic terranes elsewhere, which are more commonly between 5,000 and 10,000 m/l Cl. This is suggestive that the system has strong meteoric recharge.

As the wells were drilled with mud and aerated mud in their production zones, there are fish in BEl-01 and BEL-03 and drilling mud and cuttings were disposed of down BEL-02 (none of which are conducive towards preserving permeability in the wells) the inherent permeability of the reservoir intersected by these wells and possibly the

reservoir as a whole may be at least be slightly better than the wells currently indicate.

The elevated temperatures (242°C at -200 m asl) in TCH-4 northeast of the deep wells (Figure 1) indicate that the system continues at least this far. However, this hole was not drilled deeply enough either to get into the reservoir to establish pressure relationships or to get to where temperatures are representative of the reservoir in BEL-02 or BEL-03. The other TCH holes were drilled further to the south and southeast and have significantly lower temperatures that progressively become lower for elevation towards the east suggesting that they were drilled outside of the field's productive boundary.

The problem with potentially unrepresentative reservoir temperatures in BEL-02 and BEL-03 is due to blank liner being run below the production casing, resulting in convection in the well bore for the lengths of the blank liner. This gives misleading temperature profiles, which could be misinterpreted to indicate that the top of the reservoir is higher (at sea level) and the wells are more permeable than they actually are. The continued conductive temperature profile in the reservoir below the blank liner indicates poor permeability; however the slope is less steep than that above where the blank liner is disturbing the reservoir temperature profiles. This justifies describing the deeper parts of these wells as being in the reservoir and by extrapolating the two different conductive profiles to their meeting point allows estimation of the elevation of the top of the reservoir which is about – 300 m asl in both BEL-02 and BEL-03.

The – 300 m asl estimate for the top of the reservoir is just below the elevation of the base of the conductor (as determined by the 3D MT inversion) in the area of the deep wells, as should be the case. Making a further assumption that the temperature gradient below TCH-4 is similar to that measured in the well, the same elevation of the top of the reservoir can be estimated below TCH-4, where there is a similar elevation of the base of the conductor. Therefore it is likely that TCH-4 was drilled in the vicinity of the deep reservoir and that the base of the conductor can be used to estimate where the top of the reservoir is in the undrilled parts of the system.

3. MT BACKGROUND

Good quality magnetotelluric and TDEM data at 129 stations were collected in 1996-1997 by Geosystem Srl, under contract to Bali Energy Ltd. During the same period, Geosystem occupied 438 gravity stations, and these data were supplemented by those collected by Mulyadi (1982).

The primary product at each magnetotelluric survey site is a frequency-dependent complex impedance tensor which relates the measured electric and magnetic fields. This is usually decomposed to four relatively simple parameters for the purpose of interpretation, that is, two orthogonal pairs of apparent resistivity and phase. Under 2D conditions, these are oriented parallel and perpendicular to the geological strike, and are termed respectively the TE (transverse electric) and TM (transverse magnetic) modes, a terminology inherited from radio physics.

Data quality is good at most sites, except those close to villages, where erratic power line load changes degraded low frequency data. Most sounding curves indicate the presence of a relatively shallow conductor, overlain by a surface high resistivity layer (recent volcanics); the sub-conductor structure varies significantly within the survey area.

At very long periods, the soundings show the influence of the ocean, evidenced as a steeply-climbing apparent resistivity curve at long periods. Tipper strike indicates that the geo-electric strike at 100s period is between east and north-east; the rise of tipper amplitude towards the north suggests that this is at least in part related to the Bali Sea. At shorter periods, the strike direction is more difficult to establish, for the simple reason that on a depth-scale of a few kilometers the geology is 3D. Impedance strike is consistent with the tipper data, showing that the TE mode corresponds generally to the higher of the two apparent resistivity curves and tends to be oriented NE, although in more detail it appears to wrap around a resistive core close to the area of wells BEL-01 to –03.

2.2. 3D INVERSION OF MT DATA

The overall response of the MT data is 3D, reflecting both geological structure at depths greater than a few hundred meters and also the effect of a resistive island in a conductive ocean. For this reason, the present interpretation is based on 3D inversion, where the input is the complete impedance tensor over the frequency range 100 to 0.01 Hz. The final output from the inversion is a resistivity model of the earth, which can be displayed as depth slices and as cross-sections.

The general approach to the inversion of geophysical data consists of two steps: (1) computation of a forward response and (2) modification of the model based on the differences between the observed and computed data. To be reasonably practical, this requires a fast forward code and an efficient approach to inversion.

3-D MT data are derived from measurements at Earth's surface of naturally occurring electric and magnetic fields. A standard 3-D MT dataset typically comprises four complex quantities (impedances) as a function of receiver position and frequency. The four impedances observed in 3-D MT, then, are the components of a 2 x 2 impedance tensor. Modeling of the impedance tensor entails solving Maxwell's equations in the solid earth and atmosphere using a horizontal current source in the atmosphere to represent ionospheric and magnetospheric sources. In Geosystem's modeling algorithm the earth and atmosphere are divided into rectangular blocks with the magnetic fields defined along the block edges and the electric fields defined along the normals to the block faces (Mackie *et al*., 1994). Finite difference equations are derived using this formulation. By eliminating the electric fields from the difference equations, a second-order set of equations in H are obtained. This system of equations is sparse, symmetric, and complex (all elements are real except for the diagonal elements). Its solution is obtained by use of the stabilized biconjugate gradient algorithm. Convergence is speeded up by use of a preconditioner that is the incomplete Cholesky decomposition of the diagonal sub-blocks with fill-in, plus a correction for the divergence of the magnetic field (Mackie et al., 1994). Once the E and H fields have been determined for two linearly-independent source polarizations, the impedance tensor can be computed.

Our approach to solving the 3-D MT inverse problem is based on the framework of Tikhonov regularization (Tikhonov and Arsenin, 1977). Following many previous workers in MT inversion, smooth, or 'minimum-structure', resistivity models that give acceptable fits to the observed

data are found to be the best. Such models minimize an objective function that is the sum of the normalized data misfits plus a stabilizing functional on the model space. In our inversion algorithm, the stabilizing functional is a simple second-order operator approximating the Laplacian. Thus, solutions are models with minimum spatial variability, or roughness.

The method of nonlinear conjugate gradients (NLCG) is used to minimize the objective function. Utilization of nonlinear conjugate gradients is a well-known optimization method (Fletcher and Reeves, 1959) that has been applied to a variety of nonlinear geophysical inverse problems, e.g., Ellis and Oldenburg (1994). While NLCG is a general method for optimization, it is not necessarily efficient in a computationally intensive problem like 2-D and 3-D MT inversion. The efficiency of NLCG for computing solutions of the inverse problem depends strongly on the preconditioner and the line minimization algorithm. The purpose of the preconditioner is to steer the gradient into a direction in model space which parallels the final solution as much as possible. A restriction on this goal is that applying the preconditioner can require an excessive amount of computation if it is too complicated. The preconditioner used here is based on an approximation to the Hessian matrix. The amount of computation needed to solve the system is less than one forward function evaluation and thus adds little overhead to the algorithm. While the line minimization is only a one-dimensional problem, it still requires the computation of at least one forward problem, which in 3-D MT is computationally demanding. It is thus very important to use an algorithm that does a reasonable job of minimizing the objective function in the current search direction with as few trials as possible. Algorithms such as that in Press *et al*. (1992) do not achieve this goal. In Geosystem's 3-D MT algorithm, a line minimization algorithm is used that is basically a univariate version of the Gauss-Newton method. While details of this algorithm are given in Rodi and Mackie (2001), the important result of this algorithm is that each step of the line minimization iteration requires the equivalent work of only three MT forward calculations (the real one and two pseudo ones). An additional efficiency is the choice of the stopping criterion. It ensures that, when the forward problem is well-approximated by its linear approximation, each line minimization converges in a single step.

The net result is that the observed 3D data (each element of the impedance tensor, at each frequency used) can be inverted to give a smooth 3D model. The method is efficient and fairly fast: inversions of modest sized models typically take a day or less to compute on fast Alpha computers.

2.1. Smooth 3D inversion

Several 3D inversion runs were made, all of which began either with a uniform half space or one in which the conductive ocean was added to the north and south. The final 3D inversion used a mesh which extended about 45km beyond the edges of the survey grid. The cell dimensions within the grid were 500 x 500m horizontally, in the survey area, and 50 to 1700m vertically, increasing by a factor of 1.3 to the maximum grid depth of 44 km. The starting model incorporated the topography to the edge of the model space (2130 m a.s.l.), and the entire earth was given a starting resistivity of 20 Ωm, except for the ocean, to which a resistivity of 0.3 Ωm was assigned.

3. INTERPRETATION

An overall pattern of shallow high resistivities above a conductive layer that domes around a moderate resistivity core, similar to that found in andesitic terranes elsewhere (Anderson *et al*., 2000) is found. There are however some complexities to the overall pattern, the interpretation of which may provide greater understanding of the system.

Section NE2 (Figure 2) on which BEL-02, BEL-03 and TCH-4 can be projected to provide control over the location of the potentially exploitable resource (at least in terms of temperature), shows an asymmetric distribution of the shallow conductor. Towards the southwest the conductor becomes thicker and more conductive, with a deeper base. This is the typical pattern of the margin of an active geothermal system in an andesitic terrane. Immediately to the northeast of TCH-4 the conductor becomes less conductive and thins, with the < 10 Ωm layer disappearing. Below where the < 10 Ωm layer disappears there is an up doming in the resistivity contours. Continuing to the northeast the < 10 Ωm layer reappears as part of a thicker conductor that has a deeper base, and lower conductivities.

As there is a gravity high in this area (Figure 3) it is unlikely that the thicker conductor is a clay rich sedimentary basin. A relatively low reduction density of 2.2 g/cc has been used as this produced the least match with topography and is consistent with the very vesicular if not scoriaeous nature of the caldera fill drilled in the coreholes.

In fact the thicker conductor looks very much like the margin of a geothermal system in an andesitic terrane. Whether it is part of the active system is another matter. The overall higher shallow and northeastern marginal resistivities in combination with the deeper lower resistivities are suggestive that there has been cooling and possibly a consequent kaolinite overprint. Kaolinite is less conductive than the smectite of conductive caps, but more conductive than the alteration minerals (feldspars, amphibole and biotite) of the deep parts of the reservoirs of active geothermal systems in andesitic terranes; conductivity also decreases with temperature (Ussher et al., 2000).

Kaolinite overprints are the mark of the late stage collapse of hydrothermal systems, documented from epithermal gold deposits (Simmons *et al*., 2000). It is thus interpreted that there are at least two geothermal systems inside the Bratan caldera; the currently drilled active system that extends to TCH-4 and an older, colder system in the northeast. As this northeast system is extremely unlikely to be drilled - the northeast is a culturally and environmentally sensitive area, let alone it being an unattractive target if this interpretation is true - this interpretation is unlikely to be clearly tested. Nevertheless, there is potential to use this area as an example of an old system in order to refine the interpretation of MT surveys of geothermal systems elsewhere.

For example an MT section lines (SE5; Figure 4) that covers the western part of the Bratan caldera also contains a gap in the < 10 Ωm layer, but the doming in the underlying resistivity contours, the overall decrease in resistivity at depth and the absence of a well defined boundary structure that marks the northeastern feature are absent. A similar interpretation can therefore not be made.

An increase in the resistivity of the conductor due to kaolinite overprinting has been noted in the Wayang Windu geothermal system (Bogie *et al*., 2008), and it has been confirmed by an extensive XRD study (Abrenica *et al*., in

prep). However, at Wayang Windu, this overprint is not due to a late stage collapse, but to the boiling off of the system, which has produced extensive steam capping with an overlying condensate zone in which the kaolinite has formed in response to the elevated gas flux from extended boiling. There is also a severe misfit between the interpreted conditions of formation of the observed mineral assemblages in the steam reservoirs and the actual conditions. The PT conditions in the wells at Bedugul and the mineralogy (Muliyadi et al., 2005) do not indicate the presence of a steam capping and there is a good fit between interpreted conditions of formation of the alteration minerals and measured conditions that doesn't support a similar interpretation in this case.

If the resistivity pattern just below the interpreted top of the reservoir at -500 masl is considered in plan (Figure 5) the northeastern feature can be clearly seen as the < 23.8 Ωm blob in the northeast. The northwestern parts of section SE5 can be seen to part of a southeast trending zone that runs in towards the conductive layer. This may represent the recharge zone, where temperatures are insufficient to form a very conductive shallow layer. The upflow would then be located beneath the conductive layer where temperatures are higher. There is however very little variation in the elevation of the base of the conductor in this area to exactly locate the upflow, which may mean that the upflow is broad.

For recharge waters to inflow requires that there is an outflow. A southeast trending moderate resistivity zone (Figure 5) in the southeast lies parallel to, but is offset from the recharge zone, has strong support for being the outflow because the majority of the system's surface features lie in this general direction (Hochstein *et al*., 2005).

In addition to the strong northeast trend in the gravity high and location of the younger volcanic centers, the MT interpretation requires the presence of some major southeast trending structures. This is entirely consistent with the regional structural pattern of northeast and southeast trending conjugate strike slip faulting in response to compression from normally orientated subduction (Whitaker *et al*., 2000). The upflow could thus be located at the intersection of a conjugate pair, but this may be too localized. Another possibility is that given their strike slip nature, the offset between the two interpreted southeast trending structures is a pull-apart feature. It could provide a strong locus for intrusion to provide a heat source and for the later development of structural permeability in the form of NNE striking normal faults inside the feature, to produce a broad upflow.

A possible interpretation of such a pull-apart feature is shown in Figure 7 on the resistivity slice at – 1000 m asl; further NNE striking normal faults are likely to parallel the side of the basin. If this interpretation is correct, BEL-01 was drilled outside of the pull-apart feature, but is close enough to still be hot because of the magmatic intrusion up the feature. BEL-02 and BEL-03 were drilled near parallel to the NNE faults. Since pressure relationships indicate that BEL-02 is closest to the upflow, the upflow may be strongest up the northeast boundary of the pull-apart feature, which is consistent with the interpreted recharge from the northwest. There is then southerly flow in the pull-apart feature to link to an outflow to the southeast.

4. DEVELOPMENT IMPLICATIONS

It is possible that permeability in the Bedugul field is best (if not largely limited to) within an interpreted pull-apart feature. If this is the case, the exploitable resource will be found somewhere inside the feature. As the pull-apart feature is interpreted to be receiving cool recharge on one side and have a possibly cooling outflow on the other side, not all the pull-apart feature may represent exploitable resource.

However, the current knowledge of the distribution of high temperatures from the deep wells is sufficient to indicate that a sizeable resource is present. If the interpreted pull-apart basin is present there is also an expectation of highly permeable wells providing they are drilled in the right part of the pull-apart feature at appropriate orientations.

5. CONCLUSIONS

A 3D MT inversion can be interpreted to indicate that two geothermal systems are present within the Bratan caldera; an older, possibly colder one to the northeast and a younger, exploitable system in the southwest. Both are associated with a gravity high in a zone of northeast trending resurgent volcanism.

The southwest system appears to be structurally localized by offset southeast trending features conjugate to the northeast trend and may be forming a pull-apart feature that controls the location of the systems upflow, recharge and outflow.

Permeability may be localized within the pull-apart feature, and since the reservoir is deep, the cooler parts of the basin where there is recharge and outflow may not be exploitable. This may limit the overall exploitable resource size, but what resource is present is still likely to be substantial in size and to be of high quality.

REFERENCES

Abrenica, A.B., Harijoko, A., Kusumah, Y.I. and Bogie, I. Characteristics of hydrothermal alteration in part of the northern vapour-dominated reservoir at the Wayang Windu geothermal field, West Java. In preparation for WGC2010.

Anderson, A., Crosby, D. and Ussher, G.N. Bulls-eye – simple resistivity imaging to reliably indicate the geothermal reservoir. Proceedings WGC2000: (2000) 909-914.

Bogie, I., Kusumah, Y.I. and Wisnandary, M.C. Overview of the Wayang Windu geothermal field, West Java, Indonesia. Geothermics 37 (2008): 347-365.

Fletcher, R. and Reeves, A. M. Function minimization by conjugate gradients. Computer J., 7, (1959) 149-154.

Geosystems SrL Interpretation of Magnetotelluric Data, Bedugul, Bali, Republic of Indonesia. A report for Bali Energy Ltd. (2004).

Hochstein, M. P., Mulyadi R. and Joenos E. J. The Bedugul Geothermal Field, Bali (Indonesia). IGA News 59: (2005) 12-13.

Mackie R.L., Rodi, W. and Watts, D.M. 3-D magnetotelluric inversion for resource exploration: paper PF3.3, Extended Abstracts, Ann, Mtg. SEG, San Antonio (2001).

Mulyadi. Exploration of the Bratan Geothermal Prospect, Bali. MSc Thesis, University of Auckland (1982).

Mulyadi, R., and Hochstein, M.P. Exploration of the Bratan Caldera geothermal prospect (Central Bali).

Proceedings NZ Geothermal Workshop 1981, Univ. of Auckland, (1981) pp. 189-193.

Mulyadi, Edwin J. Joenoes, E.J. and Ni Made Widiasari, N.M. Bedugul Geothermal Prospect and Developments Proceedings World Geothermal Congress 2005 Antalya, Turkey.

Press, W.H., Teukolsky, S.A., Vetterling, W.T., and Flannery, B.P. Numerical Recipes in FORTRAN: The Art of Scientific Computing Second Edition, Cambridge University Press. (1992)

Rodi, W. and Mackie, R.L. Nonlinear conjugate gradients algorithm for 2-D magnetotelluric inversion, Geophysics, 66, (2001), 174.

Simmons, S.F, Arehart, G., Simpson, M.P., Mauk, J.L. Origin of massive calcite veins in the Golden Cross Low-Sulfidation Au-Ag Epithermal deposit, New Zealand. Economic Geology 95: (1999) 99-112.

Soetantri, B. and Prijanto. Assessment of the reservoir potential of Bali Geothermal Field, Indonesia. Transactions (3rd) Circum-Pacific Energy and Mineral Resources Conference, (1982) pp.459-464.

Tikhonov, A.N. and Arsenin, V.Y. Solutions of Ill-Posed Problems, V.H. and Sons: Washington, D.C. (1977).

Ussher, G. N., Harvey, C., Johnston, R. and Anderson, A. Understanding the resistivities observed in geothermal systems. Proceedings World Geothermal conference 2000: 1915-1920.

J.M. Whittaker, J.M., Müller, R.D, Sdrolias, M., and Heine, C. Sunda-Java trench kinematics, slab window formation and overriding plate deformation since the Cretaceous. Earth and Planetary Science Letters 255 (2007) 445–457.

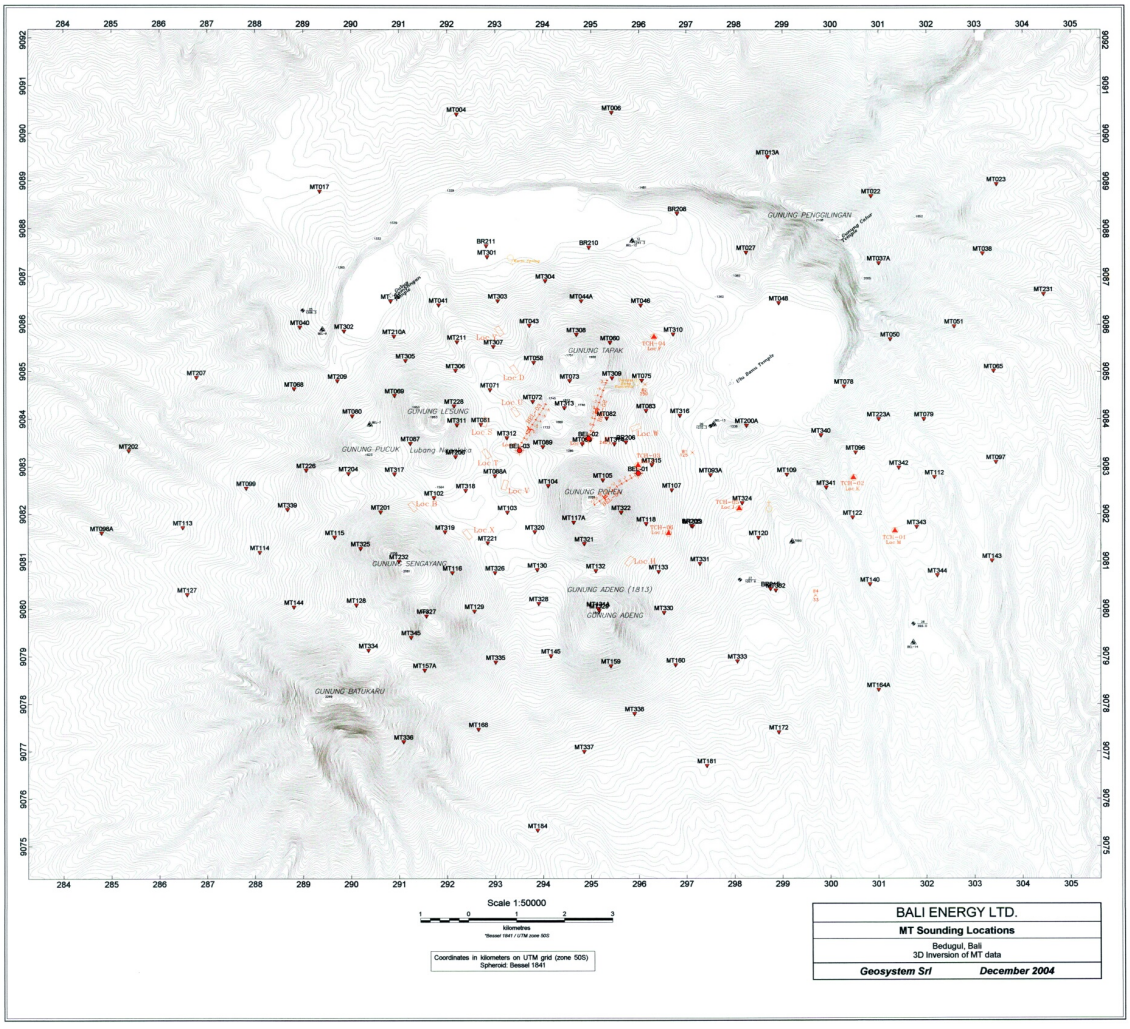

Figure 1: Location map.

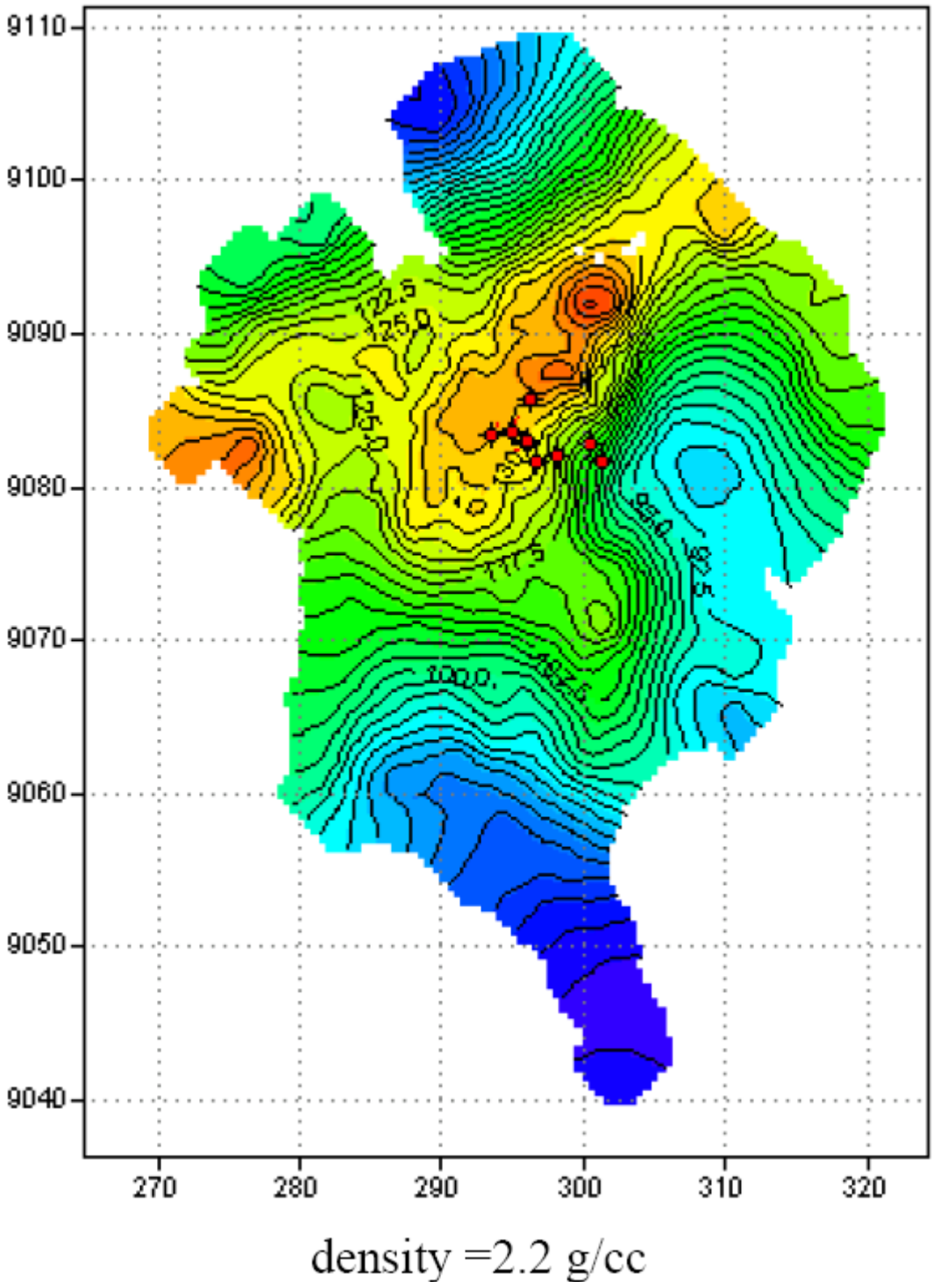

Figure 2: Gravity map.

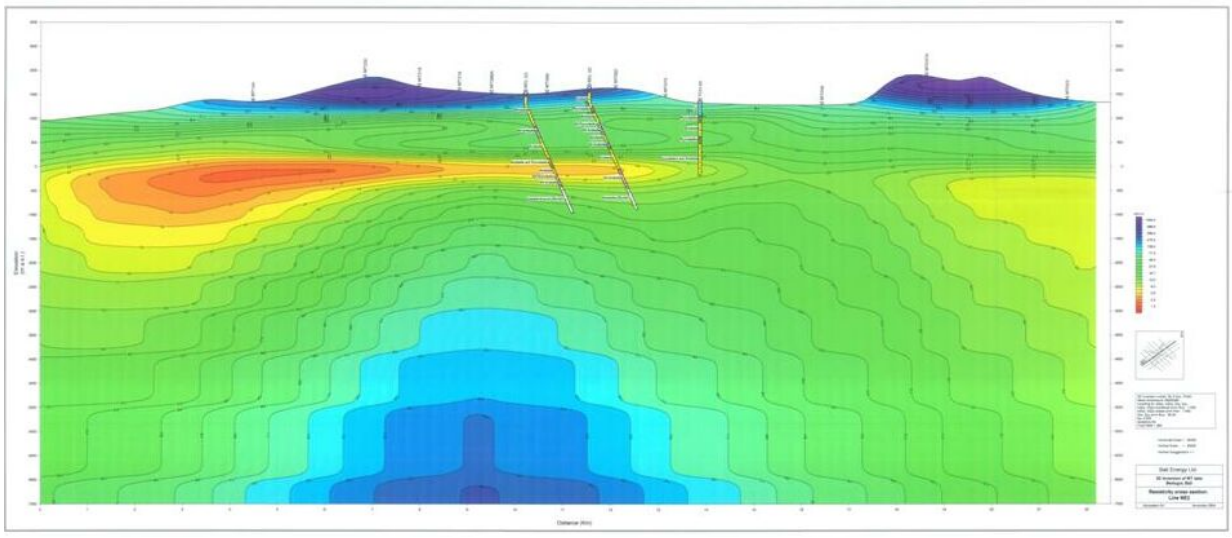

Figure 3: MT resistivity cross section NE2.

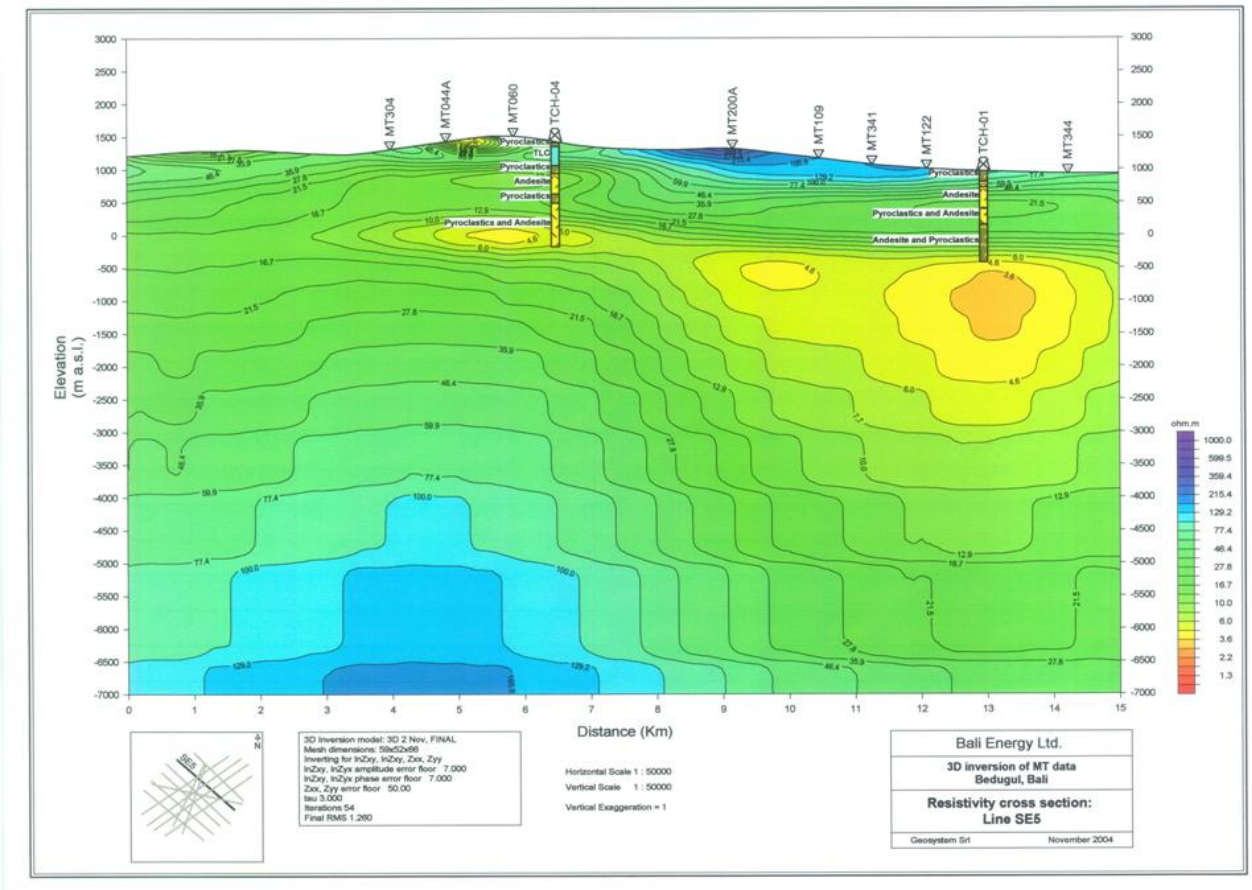

Figure 4: MT resistivity cross section SE6.

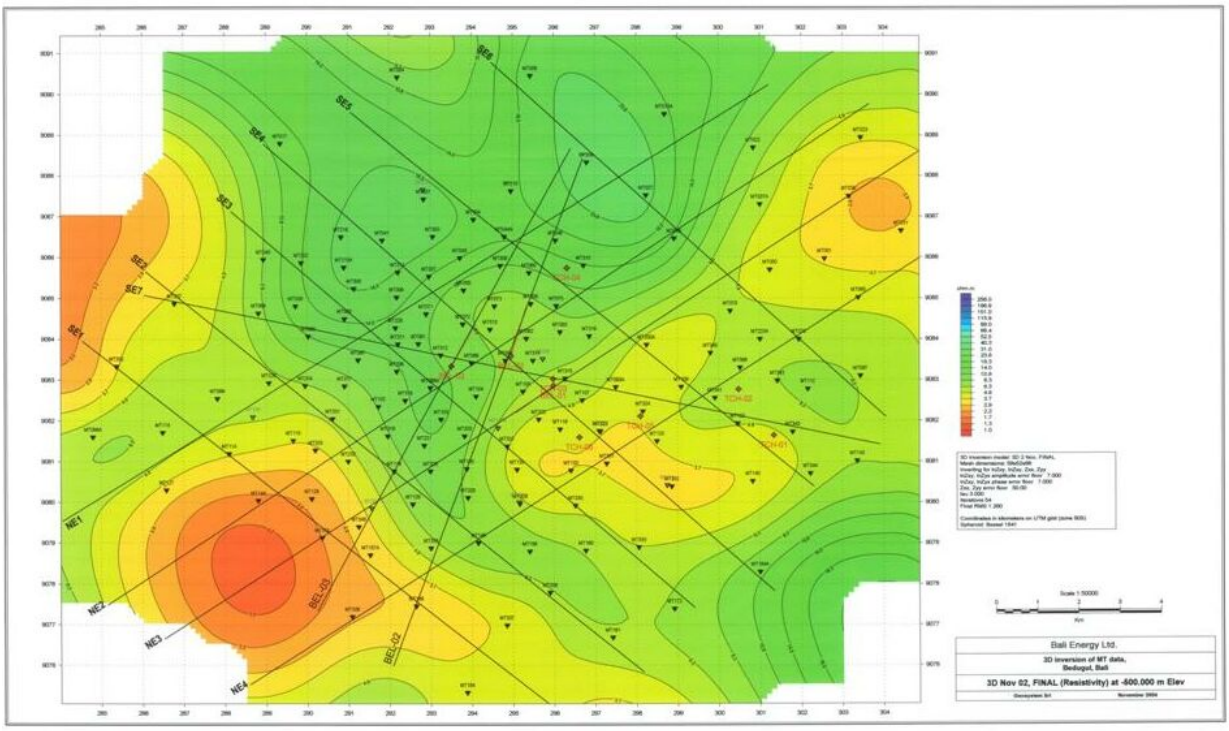

Figure 5: MT resistivity slice at – 500 m asl.

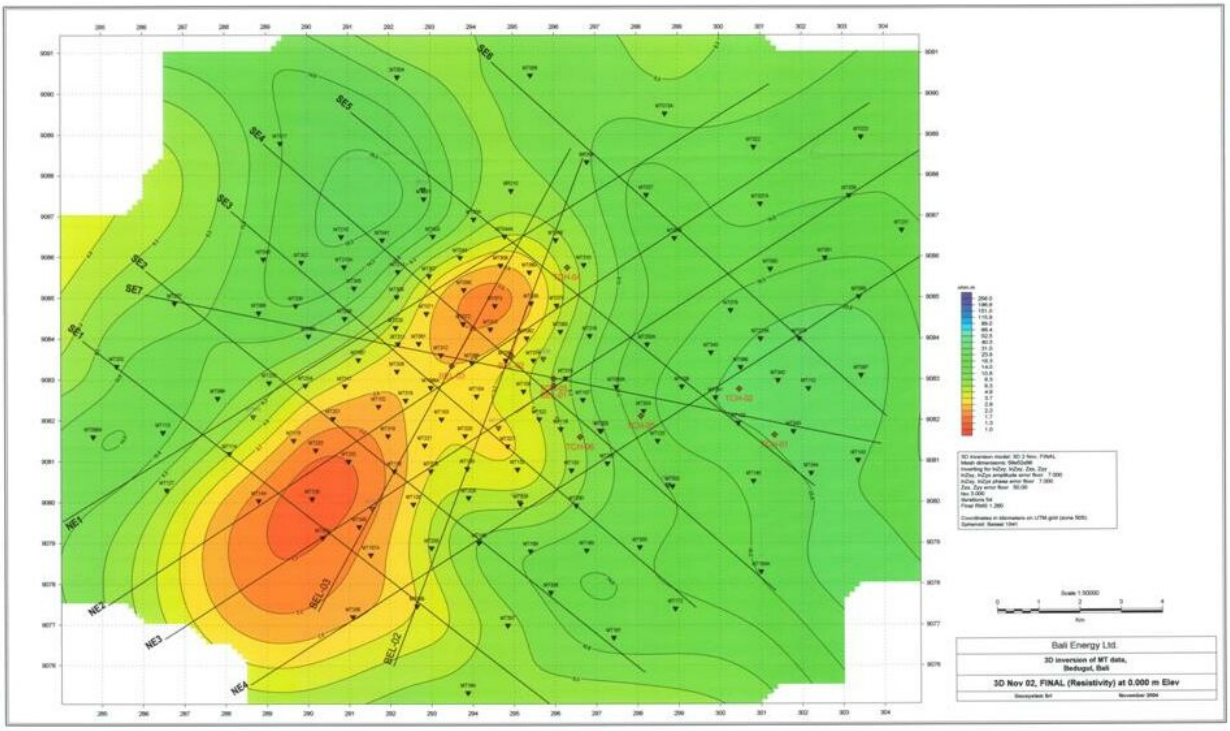

Figure 6: MT resistivity slice at – 0 m asl.

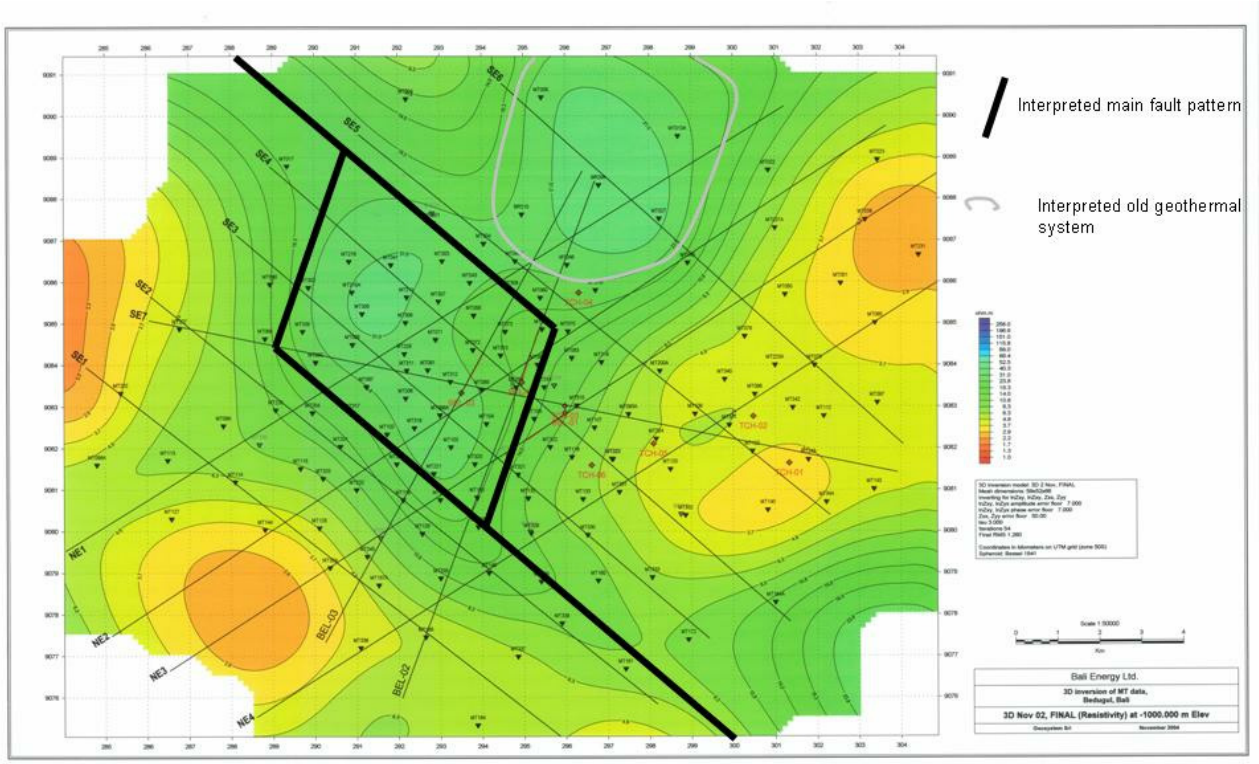

Figure 7: MT resistivity slice at – 1000 m asl with interpreted main fault pattern and old geothermal system indicated.